

The membrane fusion events in degranulating guinea pig eosinophils

M. Lindau*, O. Nüsse†

Abt. Biophysik, Freie Universität Berlin, Arnimallee 14, D-1000 Berlin 33, FRG

J. Bennett

Department of Anatomy and Cell Biology, St Mary's Hospital Medical School, Norfolk Place, London W2 1PG, UK

and O. Cromwell

Department of Allergy and Clinical Immunology, National Heart and Lung Institute, Dovehouse Street, London SW3 6LY, UK

*Author for correspondence at Abt. Molekulare Zellforschung, Max-Planck-Institut für medizinische Forschung, Jahnstrasse 29, D-6900 Heidelberg, FRG

†Present address: Department of Medicine, Brigham and Women's Hospital, 75 Francis Street, Boston, MA 02115, USA

SUMMARY

We have investigated the granule fusion events associated with exocytosis in degranulating peritoneal guinea pig eosinophils by time-resolved patch-clamp capacitance measurements using the phase detector technique. Intracellular stimulation with micromolar calcium and GTP γ S induces a 2- to 3-fold capacitance increase. The main phase of the capacitance increase occurs after a delay of 2-7 minutes and is composed of well-resolved capacitance steps. The number of steps is very close to the number of crystalloid granules contained in a resting cell and the step size distribution with a peak at 9 fF is in excellent agreement with the granule size distribution determined by electron microscopy. The individual granules thus fuse sequentially with the plasma membrane. The stepwise capacitance increase is frequently preceded by an apparently continuous capaci-

ance increase which consists of steps smaller than 4 fF, indicating exocytosis of small vesicles as distinct from crystalloid-containing granules. In some cases the time course of the opening of individual fusion pores could be recorded, and this revealed metastable conductance states below 300 pS but random fluctuations at higher conductance levels. This behaviour suggests that the small fusion pore might be a protein structure similar to an ion channel, which becomes a continuously variable lipid pore at higher conductances. In some cells a significant capacitance decrease was observed which is apparently continuous, suggesting a process of membrane uptake by endocytosis of small vesicles.

Key words: eosinophil, exocytosis, fusion pore, capacitance

INTRODUCTION

The great importance of eosinophils in health and disease has been well recognized (Kay, 1985). However, little is known about the mechanisms of the secretory process in these cells (Spry, 1988). We have recently shown that intracellular application of the non-hydrolysable GTP analogue GTP S stimulates eosinophil secretion associated with a 2- to 3-fold increase in membrane capacitance (Nüsse et al., 1990; Sceppek et al., 1991). This increase is assumed to reflect a proportional increase in membrane area, suggesting that these cells release the granular material through an exocytotic mechanism. In guinea pig eosinophils capacitance steps of 7-20 fF were observed (Nüsse et al., 1990), indicative of discrete granule fusion events during the main phase of the degranulation.

We have now investigated the fine structure of the capacitance changes during guinea pig eosinophil degranulation in more detail. In the present work we demonstrate the sequential exocytosis of individual crystalloid granules in

response to intracellular application of GTP S. We also show the time course of formation and expansion of individual fusion pores associated with fusion of single specific eosinophil granules. In addition to exocytosis of this well-characterised granule type, exocytosis as well as endocytosis of small vesicles is observed.

MATERIALS AND METHODS

Cell preparation

Dunkin Hartley guinea pigs (>600 g) were given a minimum of 5 intraperitoneal injections of 1 ml of sterile horse serum at 3-day intervals. Animals were killed by CO₂ asphyxiation 16 h after the final injection and peritoneal cells were collected by lavage with 40 ml saline (0.15 M) containing 10 units/ml preservative-free heparin (Paines and Byrne Ltd, Greenford, UK). The cells were washed twice with HBSS containing deoxyribonuclease I (30 μ g ml⁻¹) and BSA (2.5 mg ml⁻¹) and were then resuspended in 3 ml HBSS (Hanks' balanced salt solution) and layered onto 2 discontinuous Percoll gradients comprising 2 ml steps of 1.070,

1.080, 1.085, 1.090, 1.095 and 1.100 g ml⁻¹ in 15 ml conical tubes. The gradients were centrifuged (1500 g, 20 min at 20°C) and eosinophils were recovered from the 1.095/1.100 g ml⁻¹ interface, with a minimum purity of 98% and typical yields of 3×10^7 to 4×10^7 cells per animal as judged by toluidine blue/light green staining (Kimura et al., 1975). Macrophages were the contaminating cell type. Exclusion of trypan blue was greater than 96%.

Patch-clamp experiments were conducted in Berlin using cells shipped from London via DHL International Ltd (Couriers; Hounslow, UK). For this purpose cells were transferred to Medium 199 (Gibco, Paisley, UK) containing 5% FCS Myclone Plus (Gibco), penicillin G (50 units/ml and streptomycin (50 µg/ml). Cells reached their destination within 30 h and were kept in the same culture medium for up to 96 h, during which time no significant differences in responsiveness were observed.

Patch-clamp capacitance measurements

About 100 µl of cell suspension were transferred to Petri dishes with a window formed from coverslip glass sealed into the base. After a few minutes to allow the cells to settle on the glass the dish was perfused with standard external saline (see below). The whole-cell configuration of the patch-clamp technique was used to dialyse the cells with internal solutions of different composition. The internal solutions contained 125 mM potassium-L-glutamate, 10 mM NaCl, 7 mM MgCl₂, 1-2.5 mM Na₂ATP, 5 mM EGTA, 4.5 mM CaCl₂, 20 µM GTP S and 10 mM HEPES/NaOH, pH 7.2-7.3. In all experiments the bath solution contained 140-145 mM NaCl, 5 mM KCl, 2 mM CaCl₂, 1 mM MgCl₂, 10 mM HEPES/NaOH, pH 7.2, 6-20 mM glucose. All experiments were done at room temperature.

A continuous 800 Hz, 20 mV (rms) sine wave was given as the command voltage of the patch-clamp amplifier (EPC 7, List Electronics, Darmstadt, FRG) operating in the voltage clamp mode and the current output signal was fed into an integrating two-phase lock-in amplifier (Lindau and Neher, 1988; Breckenridge and Almers, 1987a). After patch disruption the capacitance of the cell was compensated and the phase error of the lock-in was automatically determined by switching a 1 MΩ resistor into the connection between the bath electrode and the ground input of the head stage (Fidler and Fernandez, 1989). The lock-in outputs were sampled by the computer (PDP 11/73 with laboratory interface) and the traces reflecting changes in either membrane capacitance (C_m) or membrane conductance (G_m) and access resistance (R_A) were calculated online (Lindau et al., 1992). With this method a manual phase adjustment was not necessary. Only the capacitance was manually compensated and the recordings could be started within 10-20 s after patch disruption. The lock-in outputs were sampled every 15-50 ms and the phase was tracked every 250 data points. During the experiment the capacitance compensation was readjusted when the current signal approached saturation of the amplifier. We have realigned the consecutive sections of the capacitance and conductance trace by shifting the section after phase or compensation adjustment so that the beginning coincides with the value expected from extrapolation of the section before the adjustment. With this method it was possible to reconstruct the time course of the whole degranulation at high resolution.

Electron microscopy and morphometric analysis

Cells were fixed in suspension in HBSS, using 2.5% glutaraldehyde followed by 1% osmium tetroxide. Following dehydration and embedding in Araldite resin, thin sections (70-90 nm) were post-stained in uranyl acetate and lead citrate, and examined in the electron microscope. The size s of individual granule profiles was quantified as the average of the long and short axes of that profile. The size distribution was determined as the number of

profiles n_i having a size s_i . The total number of granules per cell was estimated by counting the profiles visible in 12 sections. There was a random distribution of sections with respect to the proportion of the cytoplasm which was covered by the nucleus. The average fraction of the section area covered by the nucleus was thus equal to the average fraction of cell volume taken up by the nucleus. The total area of the sections was determined with a balance by cutting out the cells and the average density of granule profiles per µm² (N_A) was calculated. Approximating the granule profiles by circles with mean radius $r_i = s_i/2$, the number of crystalline granules per unit volume N_V was calculated from the profile size distribution in thin sections as $N_V = 1 / \int p_i / r_i$ (Bach, 1967), where p_i is the absolute frequency per µm² of profiles with mean radius r_i ($p_i = N_A n_i / n_i$).

Treating the granules as approximate spheres the capacitance step size distribution was converted to a granule diameter distribution, assuming specific capacitance values between 0.6 and 1.0 µF/cm². Using this distribution we have calculated the expected cross-section distribution for sections with a thickness $T = 70$ nm, as described by Bach (1967).

RESULTS

Two distinct phases of capacitance increase

Fig. 1A shows a phase-tracking reconstruction of the membrane capacitance obtained from a guinea pig eosinophil stimulated with intracellular saline containing 20 µM GTP S and ~1.5 µM free calcium. The recording starts 12 s after patch disruption. The trace shows four calibration marks (black dots) where the compensation was transiently reduced by ~90 fF. These simulations of a known capacitance increase generated changes of rather constant size throughout the recording, demonstrating that the calibration factor did not change significantly during the experiment. An obvious feature of Fig. 1A is that the capacitance increases in two distinct phases. The initial increase shows no detectable latency whereas the second phase commences after a delay of several minutes. The temporal separation of the two processes indicates that they may be controlled by different mechanisms.

The labelled sections of Fig. 1A are expanded in B and C. Although the capacitance changes by ~150 fF during 30 s in both sections and the overall slope is thus very similar in B and C, the fine structure of these capacitance changes is very different. In the early part (B) there may be one step of ~7 fF whereas all other steps which may underly this increase are smaller than 4 fF. In contrast, the second phase (C) is almost completely composed of steps between 7 and 20 fF. In this cell the total capacitance change was 3.4 pF, with 2.5 pF due to large steps and 0.9 pF due to small steps of less than 4 fF.

A continuous capacitance increase preceding the stepwise increase was always observed. However, the amplitude was very variable. 20-30 s after patch disruption the slope was 5 ± 3 fF/s (s.d., $n = 8$). The amplitude of the graded increase from 20 s on was 0.48 ± 0.31 pF (s.d., $n = 8$). The amplitude of the stepwise increase was much less variable (2.65 ± 0.28 pF, s.d., $n = 4$).

When the guanine nucleotide GTP S was omitted from the pipette solution the delayed stepwise capacitance increase was never observed. However, a rapid continuous

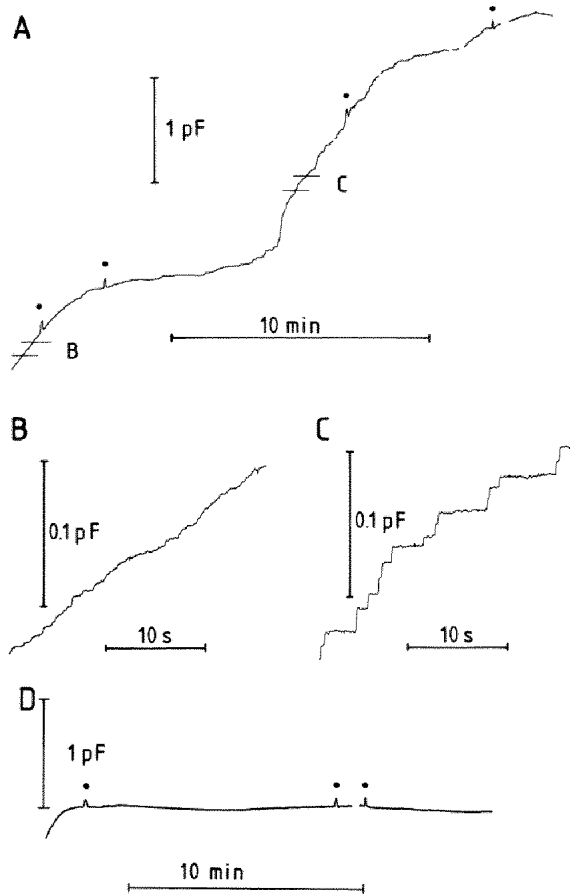


Fig. 1. (A) High-resolution capacitance record of a degranulating eosinophil stimulated by intracellular application of 20 μM GTP S. The capacitance compensation was transiently reduced by 90 fF at the points marked by a black dot. The labelled sections are shown on an expanded scale in B and C. (D) Time course of membrane capacitance recorded from a cell dialysed with the same pipette solution as in (A) but without GTP S.

capacitance increase occurred even in the absence of GTP S (Fig. 1D), but the increase was generally smaller (0.22 ± 0.17 pF, s.d., $n = 3$). The probability that the difference in the amplitude in the presence and absence of GTP S is significant is 80% (*t*-test).

The capacitance step size distribution

The step size distribution, constructed from measuring 939 steps in 6 cells is shown in Fig. 2A. The peak of the step size distribution is close to 9 fF and the mean step size is 15 fF. Fig. 2B shows the size distribution of the 233 capacitance steps during the second phase of the cell shown in Fig. 1A. It appears that the shape of the distribution is very similar. The size distribution is thus a feature of the individual cell and does not reflect variability among individual cells. Normalizing the step size distribution to the total average stepwise increase of 2.65 pF yields an average number of 210 capacitance steps per cell. Assuming spherical geometry for the granules and a specific capacitance of $1 \mu\text{F}/\text{cm}^2$ the step size distribution dn/dC_m (Fig. 2A) can be converted into the granule size distribution dn/dD , where D is the granule diameter. This size distribution is shown

in Fig. 2C and shows a sharp peak at 520 nm. To compare these data with morphometric data from electron microscopy (EM) of thin sections we have calculated the expected distribution of intersecting circles from the data of Fig. 2C (Fig. 2D, continuous line).

The granule size distribution

Fig. 3 shows an EM section of a guinea pig eosinophil. Owing to the crystalloid core the shape of the granules is rather irregular and the cross-sections appear mainly as elongated structures. Since the exact shape of the granules is unknown we are unable to give an exact quantitative comparison with the capacitance step size distribution. We have instead calculated the average of the long and short axis of each of 349 profiles contained in 12 sections and the frequency distribution of these values denoted as 'profile size' is also given in Fig. 2D (vertical bars). The total area of the 12 sections was $480 \mu\text{m}^2$, giving a density of 0.73 profile per μm^2 and an estimate of ~ 190 granules per cell. The size distribution expected from the capacitance steps and the measured profile size distribution are very similar. The slight shift of the peak may result from the non-spherical granule shape but could also reflect a lower specific capacitance of the granule membrane. Assuming a specific capacitance of $0.6\text{--}0.7 \mu\text{F}/\text{cm}^2$ (Fig. 2D, dotted and broken lines) leads to excellent agreement of the two distributions. Occasionally we have observed very large capacitance steps of up to 110 fF. Such a step would correspond to a spherical granule with a diameter of 1.8–2 μm . Among the 349 granule profiles we observed one with a mean size of 1.55 μm ; 5% of the capacitance steps were larger than 30 fF, which would correspond to granules with a diameter exceeding 1 μm . This should be compared with the value of 3% of the measured granule profiles which were larger than 1 μm . Given the fact that the profiles are usually smaller than the granules, since any section is unlikely to be exactly equatorial through the granule, the size and frequency of the large capacitance steps are in rather good agreement with the size and frequency of large granules in unstimulated cells.

The opening of individual fusion pores

In some recordings we have observed apparently irregular capacitance fluctuations as well as downward steps in the capacitance trace. Fig. 4A shows such events during degranulation. Most capacitance changes are regular on-steps (arrows) as expected for addition of the granule membrane to the plasma membrane. There is, however, also a period with apparently irregular fluctuations (horizontal bar) and a capacitance off-step is seen at the asterisk. This part is shown on an expanded time scale in Fig. 4B (top trace). Fluctuations in the capacitance trace can be caused by fluctuations in the fusion pore conductance G_P connecting the interior of the granule with capacitance C_G to the extracellular space (Breckenridge and Almers, 1987a,b; Zimmerberg et al., 1987; Alvarez de Toledo and Fernandez, 1988; Spruce et al., 1990).

When the pore conductance is small, the capacitance trace yields $Y_2 = C_G / \{1 + (C_G/G_P)^2\}$ rather than C_G . In Fig. 4B (top trace) the initial capacitance is indicated by

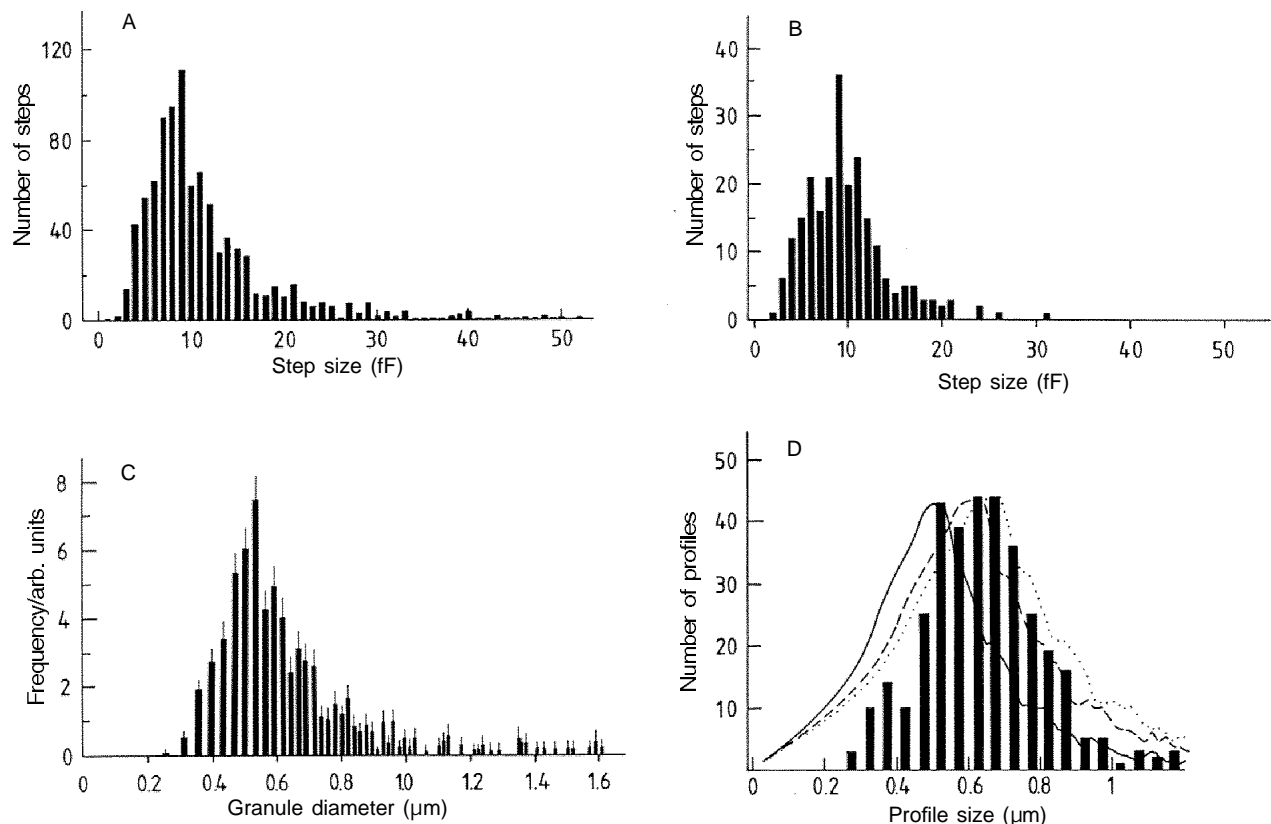


Fig. 2. (A) Capacitance step size distribution obtained from 939 steps measured in 6 cells. (B) Step size distribution obtained only from the cell of Fig. 1. (C) The distribution of (A) converted to a granule diameter distribution, assuming spherical geometry and a specific capacitance of $10 \text{ fF}/\mu\text{m}^2$. (D) The frequency distribution of the size of 349 granule profiles determined from electron micrographs as the mean between long and short axes. The expected profile diameter distributions calculated from the data of (A) are drawn, assuming specific capacitances of $10 \text{ fF}/\mu\text{m}^2$ (continuous line), $7 \text{ fF}/\mu\text{m}^2$ (broken line) and $6 \text{ fF}/\mu\text{m}^2$ (dotted line).

the continuous line and the granule capacitance C_G is assumed to be equal to the difference between the continuous and the broken line. The time course of the fusion pore conductance can thus be calculated from the measured Y_2 trace according to $G_P = C_G \frac{Y_2}{(C_G - Y_2)}$ and is shown in the second trace of Fig. 4B. The fusion starts with a fusion pore conductance around 170 pS. The conductance then decreases to a very small value for 160 ms before it increases and attains a conductance exceeding 500 pS. However, after 1.5 s the fusion pore again closes completely for 800 ms until it opens again and stays open. If the interpretation is correct, that the fluctuations in the capacitance trace are solely due to fluctuations in the conductance of the fusion pore (G_P), then the conductance trace should display a signal $Y_1 = Y_2 \cdot C_G / G_P$ as shown in the third trace of Fig. 4B. The bottom trace is the measured conductance trace, which is apparently very similar to the predicted trace, confirming that the fluctuations in the capacitance trace are indeed due to fluctuations in the fusion pore conductance with the time course shown here.

Fig. 5A-D shows four other pore-opening events analysed in the same way as described above. Here we show only the time course of the fusion pore conductances. The first event (Fig. 5A) displays behaviour reminiscent of the opening and closing of an ion channel having a conductance of 250 pS. The reversible openings suggest that a defined structure exists for ~ 3 s, which fluctuates between

the open and the closed state until the pore widens irreversibly. The opening of Fig. 5B shows a pore which rapidly attains a conductance of 180 pS and starts to expand immediately in a gradual manner. In Fig. 5C the pore also fluctuates between an open and closed state as in Fig. 5A but now the conductance of the open state is as low as 90 pS. Fig. 5D shows very different behaviour. After opening of the fusion pore in two steps via states of ~ 70 pS and ~ 180 pS conductance we see fluctuations between a relatively well-defined lower conductance level and apparently irregular levels of higher conductance. It thus appears that the fusion pore attains a minimal conductance of about 330 pS from which it repeatedly expands and contracts in a continuous manner, indicating that in contrast to the lower conductance states, the fusion pore has become a flexible structure. The expansion apparently occurs against a force keeping the pore in the narrow state. In agreement with this interpretation is the occurrence of short glitches (Fig. 5A,C) corresponding to conductance values much larger than the stable fusion pore level.

Membrane uptake following exocytosis

We have occasionally observed a significant capacitance decrease following the capacitance increase associated with exocytosis. The record of a cell showing a particularly large decline in capacitance is shown in Fig. 6A (upper trace). The recording starts ~ 20 s after the whole cell configura-

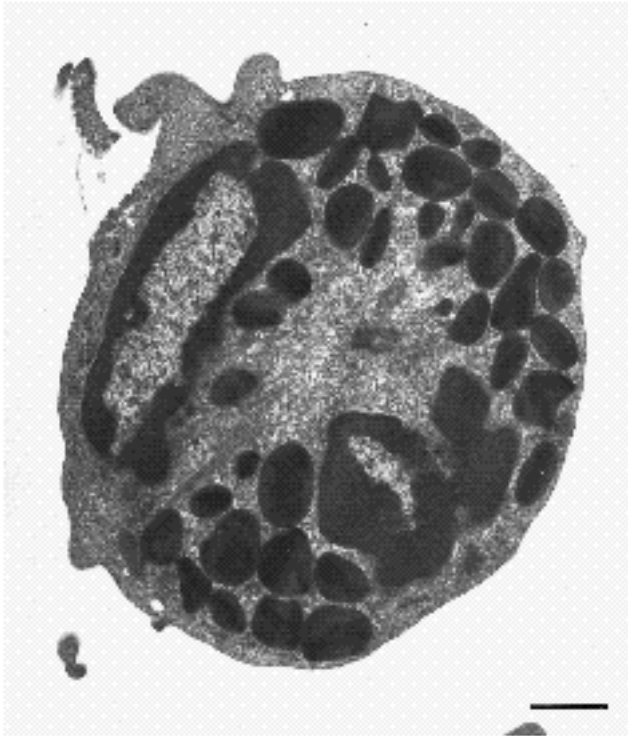


Fig. 3. Electron micrograph of an unstimulated guinea pig eosinophil. The crystalloid-containing granules can be clearly identified. Bar, 1 μm .

tion was established. As before, the rapid continuous and the subsequent stepwise phase of the capacitance increase are seen. The capacitance increased from an initial value of 3.2 pF to a maximal value of 6.1 pF as determined by the capacitance compensation before the beginning of the record and during the gap at the maximum of the capacitance trace. A capacitance decrease is already apparent after the second calibration but then the slope becomes positive again due to increased exocytotic activity. After most of the granules are fused there is an obvious decline in the capacitance, which has a value of 4.9 pF at the end of the recording.

The corresponding conductance trace (Fig. 6A, lower trace) shows periodic spikes generated by the artificial 1 M access resistance changes used for phase tracking. No corresponding spikes are seen in the capacitance trace, confirming the correct phase adjustment and separation of capacitive and ohmic changes. The conductance trace shows a slight increase due to an increase of access resistance from 11 to 13 M Ω as noted from the compensation settings.

Part of the capacitance decrease is shown in Fig. 6B on an expanded scale. The capacitance decrease appears to be continuous and at a resolution of 2 fF no off steps are seen. There are four on steps having a size of 6-18 fF, indicating that these reflect exocytosis of the last crystalloid granules. The initial slope of the capacitance decrease is about 5 fF/s, indicating that about 0.5-0.7 μm^2 of membrane are taken up per second. The absence of steps suggests that the internalised units have a membrane area of less than 0.3 μm^2 , corresponding to vesicles with a diameter of less than

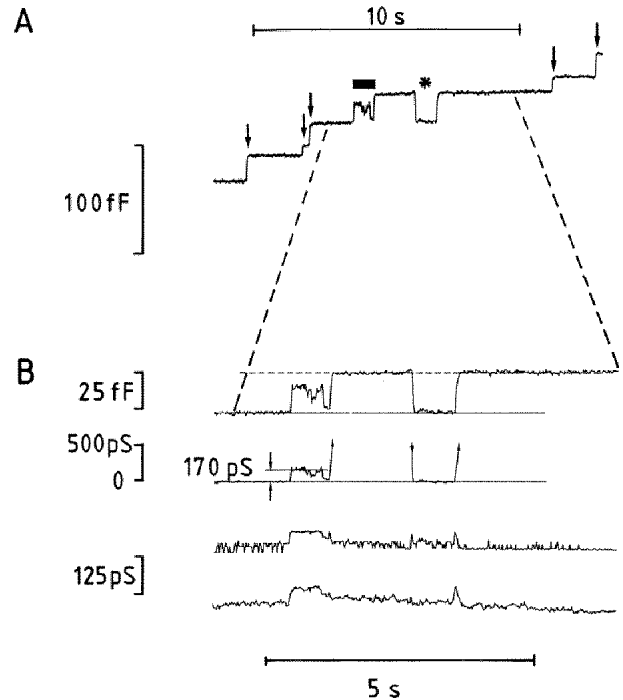


Fig. 4. (A) A section of a capacitance record showing on steps (arrows), apparently irregular fluctuations (bar) and an off step followed by an on step of the same size (asterisk). (B) The middle part is shown on an expanded scale (top trace). The continuous line indicates the capacitance of the unfused state and the broken line the capacitance for the completely fused granule. The time course of the fusion pore conductance (second trace) connecting the interior of the granule with extracellular space determined from the capacitance trace. The expected (third trace) and measured (bottom trace) of the Y_1 output of the lock-in amplifier.

300 nm. Some endocytotic activity was also occasionally observed in the absence of GTP S in cells where exocytotic fusion of crystalloid granules had not occurred, but under these conditions the rate of membrane uptake was only 0.25 fF/s.

DISCUSSION

We have investigated the fine structure of the capacitance changes associated with degranulation in guinea pig eosinophils. The experiments reveal a variety of interesting details of exo- and endocytosis in this cell type.

Sequential exocytosis of individual crystalloid granules

The main phase of degranulation stimulated by intracellular application of GTP S is a sequence of steps reflecting the sequential fusion of individual specific crystalloid-containing granules. The average number of 210 capacitance steps per cell is in very good agreement with the morphometric estimate of 190 granules per cell. The specific capacitance of the granule membranes appears to be in the range 6 to 10 fF/ μm^2 in good agreement with the most widely assumed value of 10 fF/ μm^2 for biological membranes (Cole, 1964) and the specific capacitance determined in

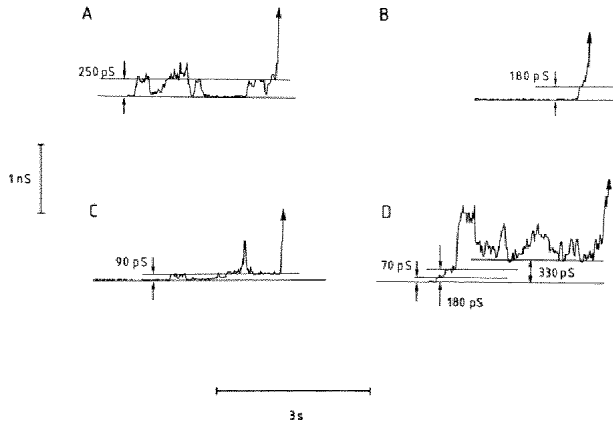


Fig. 5. The time course of four other individual fusion pore openings. The horizontal lines indicate the closed and metastable conductance states of the fusion pores.

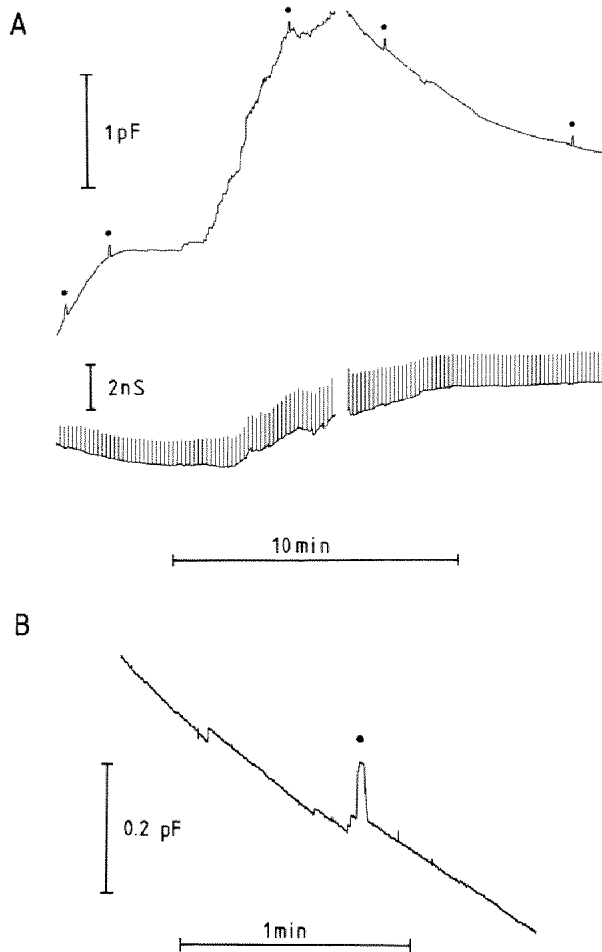


Fig. 6. (A) Time course of capacitance (upper trace) and conductance (lower trace) recorded in a cell showing a marked capacitance decrease after degranulation. The black dots denote compensation changes by 90 fF. (B) Part of the capacitance trace on an expanded scale showing a continuous capacitance decrease and some on steps due to the last exocytotic fusion events.

patch-clamp experiments for the secretory granules of murine peritoneal mast cells (Fernandez et al., 1984; Breckenridge and Almers, 1987b; Zimmerberg et al., 1987) and human neutrophils (Nüße and Lindau, 1988).

It has been suggested from electron microscopy that in horse eosinophils stimulated with the calcium ionophore A23187 several granules discharge their contents into a large cytoplasmic vacuole, which then fuses with the plasma membrane, releasing its contents through a fusion pore (Henderson et al., 1983). This would lead to a capacitance increase with the same total amplitude as in the case of sequential fusion of individual granules, but the increase would occur in a few very large steps, since inter-granule fusions of cytoplasmic membranes do not affect the capacitance of the plasma membrane. We have shown that the total number of steps is equal to the number of granules in a resting cell and the measured step size distribution agrees very well with the granule size distribution (Fig. 2). The formation of large compounds before fusion with the plasma membrane is therefore at least a rare event.

The opening of individual fusion pores

A very small number of fusion events were associated with the reversible opening and closing of the fusion pore and in such cases the dynamics of the fusion process could be followed by recording the time course of the fusion pore conductance. An interesting feature of these events is that the pore conductance may attain long-lived metastable states below 300 pS, but shows irregular fluctuations at higher conductances. This indicates that small fusion pores behave somewhat similarly to ion channels, whereas after expansion the behaviour suggests the formation of a lipidic pore. The stable states between 70 and 300 pS are in exactly the same range as the initial conductance of fusion pores in beige mouse peritoneal mast cells (Breckenridge and Almers, 1987a; Spruce et al., 1990).

A rapid capacitance increase with small unit steps

The major change in capacitance, reflecting the fusion of the crystalloid-containing eosinophil granules is frequently preceded by a rapid capacitance increase, most of which could not be resolved as a sequence of steps. For this increase of membrane area the vesicles incorporated into the plasma membrane must be smaller than 450 nm in diameter corresponding to capacitance steps generally smaller than 4 fF. The first phase of the capacitance increase can thus not be explained by exocytosis of crystalloid granules. In rat peritoneal mast cells high intracellular calcium also induces continuous capacitance changes without steps and visible degranulation. It was suggested that they may reflect Ca-dependent shifts of the equilibrium between constitutive exo- and endocytosis involving small vesicles (Almers and Neher, 1987).

It has been suggested that the contents of the crystalloid granules may be secreted by a mechanism named "piecemeal" degranulation (Dvorak et al., 1991), involving transport of small amounts of granular material to the plasma membrane by small vesicles. However, our data indicate that the number of steps as well as the size of the steps

fully account for all the crystalloid granules present in a resting cell. The continuous increase is added to the total increase, indicating that the small vesicles are not derived from the crystalloid granules.

In rat peritoneal eosinophils small granules measuring less than 500 nm diameter have been identified and characterised by their unmasked acid phosphatase (Komiya and Spicer, 1975), which was not demonstrable in the large crystalloid granules. A few small granules can be seen in electron micrographs of guinea pig eosinophils. The sections contain ~ 0.08 small granule per μm^2 with a diameter of ~ 250 nm corresponding to ~ 65 granules per cell. Exocytosis of these granules would produce a capacitance increase of less than 0.15 pF, which is too small to account for the observed first phase of the capacitance increase. It has been suggested that the small granules should be classified as secondary lysosomes, and because of their ability to take-up colloidal gold it was concluded that they were "heterophagic organelles" (Komiya and Spicer, 1975).

There is another class of granules, the so-called specific microgranules, present in eosinophils from at least 20 species including guinea pig, which measure 20-200 nm (Schaefer et al., 1973). They are more abundant during eosinophilia than when the eosinophil count is in the normal range (Zucker-Franklin, 1980). They are preferentially located at the periphery of the cell, suggesting that they may form part of the cell's secretory apparatus (Zucker-Franklin, 1980). In electron micrographs the specific microgranules appear as spheres, double spheres, dumbbell- and cup-like structures. The cup-like and coated vesicles were, however, shown to be involved in a process called microendocytosis (Komiya and Spicer, 1975) (see below). The dumbbell-like vesiculotubular structures which are present in guinea pig eosinophils (Schaefer et al., 1973) are apparently not involved in endocytosis (Komiya and Spicer, 1975) and are thus the most likely candidates to be the organelles generating the expansion in membrane area underlying the rapid phase of the capacitance change.

A capacitance decrease indicating endocytosis

Some cells show a continuous capacitance decrease, which may occur between the steps during the main phase of degranulation, but which is most obvious after degranulation is complete. Such a capacitance decrease would be expected from membrane uptake by an endocytotic mechanism. Although we cannot give a satisfactory explanation as to why endocytosis is only occasionally seen, the important point is that, if endocytosis is detectable, then the uptake occurs in the form of small vesicles.

Microendocytosis has been observed in rat peritoneal eosinophils following intraperitoneal infusion of saline or fetal calf serum (Komiya and Spicer, 1975) and is associated with the appearance of small membrane-limited structures (<100 nm) inside the cell. Among these are coated vesicles and cup-like structures that incorporate colloidal gold, classifying them as endocytotic vesicles. Such a process would manifest itself in the capacitance change as a decrease consisting of very small steps, as observed in our experiments. In human eosinophils stimulated with the calcium ionophore A23187 electron microscopy indicated exocytotic fusion of crystalloid granules with the plasma

membrane and an increased number of small granules (Henderson and Chi, 1985). While it was proposed that these structures might represent newly formed granules it has also been suggested that the small granules are the remains of crystalloid granules that have secreted most of their contents (Spry, 1988). Our results indicate that they are formed by an endocytotic mechanism of membrane reuptake. The endocytotic capacitance decrease might reflect the process of microendocytosis described above.

We thank Stefanie Wolgast for excellent technical assistance and the preparation of the figures, and Regina and Maren for cutting the cell profiles. We also thank Bastien Gomperts and Peter Tatham for critically reading our manuscript. This work has been supported by the Deutsche Forschungsgemeinschaft (Sfb 312 / B6 and LI 443/3-1) and the National Asthma Campaign.

REFERENCES

- Almers, W. and Neher, E. (1987). Gradual and stepwise changes in the membrane capacitance of rat peritoneal mast cells. *J. Physiol.* **386**, 205-218.
- Alvarez de Toledo, G. and Fernandez, J. M. (1988). The events leading to secretory granule fusion. In *Cell Physiology of Blood, Society of General Physiologists series*, vol. 43 (ed. Gunn, R. B. and J. C. Parker), pp. 333-344. New York: Rockefeller University Press.
- Bach, G. (1967). Kugelgrößenverteilung und Verteilung ihrer Schnittkreise; ihre wechselseitigen Beziehungen und Verfahren zur Bestimmung der einen aus der anderen. In *Quantitative Methoden der Morphologie* (ed. Weibel, E. R. and Elias, H.), pp. 23-45. Berlin: Springer Verlag.
- Breckenridge, L. J. and Almers, W. (1987a). Currents through the fusion pore that forms during exocytosis of a secretory vesicle. *Nature* **328**, 814-817.
- Breckenridge, L. J. and Almers, W. (1987b). Final steps in exocytosis observed in a cell with giant secretory granules. *Proc. Nat. Acad. Sci. USA* **84**, 1945-1949.
- Cole, K. S. (1968). *Membranes, Ions and Impulses*. Berkeley: University of California Press.
- Dvorak, A. M., Furitsu, T., Letourneau, L., Ishizaka, T. and Ackerman, S. J. (1991). Mature eosinophils stimulated to develop in human cord blood mononuclear cell cultures supplemented with recombinant human interleukin 5. Part I. Piecemeal degranulation of specific granules and distribution of Charcot-Leyden crystal protein. *Amer. J. Pathol.* **138**, 69-82.
- Fernandez, J. M., Neher, E. and Gomperts, B. D. (1984). Capacitance measurements reveal stepwise fusion events in degranulating mast cells. *Nature* **312**, 453-455.
- Fidler, N. and Fernandez, J. M. (1989). Phase tracking: an improved phase detection technique for cell membrane capacitance measurements. *Biophys. J.* **56**, 1153-1162.
- Henderson, W. R. and Chi, E. Y. (1985). Ultrastructural characterization and morphometric analysis of human eosinophil degranulation. *J. Cell Sci.* **73**, 33-48.
- Henderson, W. R., Chi, E. Y., Jörg, A. and Klebanoff, S. J. (1983). Horse eosinophil degranulation induced by the ionophore A23187: ultrastructure and role of phospholipase A₂. *Amer. J. Path.* **111**, 341-349.
- Kay, A. B. (1985). Eosinophils as effector cells in immunity and hypersensitivity disorders. *Clin. Exp. Immunol.* **62**, 1-12.
- Kimura, I., Moritani, Y. and Tanizaki, Y. (1975). Basophils in bronchial asthma with reference to reagin-type allergy. *Clin. Allergy* **3**, 195.
- Komiya, A. and Spicer, S. S. (1975). Microendocytosis in eosinophilic leukocytes. *J. Cell Biol.* **64**, 622-635.
- Lindau, M. and Neher, E. (1988). Patch-clamp techniques for time-resolved capacitance measurements in single cells. *Pflügers Arch. Eur. J. Physiol.* **411**, 137-146.
- Lindau, M., Stuenkel, E. L. and Nordmann, J. J. (1992). Depolarization, intracellular calcium and exocytosis in single vertebrate nerve endings. *Biophys. J.* **61**, 19-30.
- Nübe, O. and Lindau, M. (1988). The dynamics of exocytosis in human neutrophils. *J. Cell Biol.* **107**, 2117-2124.

- Nüße, O., Lindau, M., Cromwell, O., Kay, A. B. and Gomperts, B. D.** (1990). Intracellular application of GTP- γ S induces exocytotic granule fusion in guinea-pig eosinophils. *J. Exp. Med.* **171**, 775-786.
- Scepek, S., Nüße, O., Sachße, G. and Lindau, M.** (1991). Horse eosinophils: a new model system for biophysical studies of exocytosis. *Eur. J. Cell Biol.* **54**, 23.
- Schaefer, H. E., Hubner, G. and Fischer, R.** (1973). Spezifische Mikrogranula in Eosinophilen. *Acta Haematol. (Basel)* **50**, 92-104.
- Spruce, A. E., Breckenridge, L. J., Lee, A. K. and Almers, W.** (1990). Properties of the fusion pore that forms during exocytosis of a mast cell secretory vesicle. *Neuron* **4**, 643-654.
- Spry, C. J. F.** (1988). *Eosinophils: A Comprehensive Review and Guide to the Scientific and Medical Literature*. Oxford: Oxford University Press.
- Zimmerberg, J., Curran, M., Cohen, F. S. and Brodwick, M.** (1987). Simultaneous electrical and optical measurements show that membrane fusion precedes secretory granule swelling during exocytosis of beige mouse mast cells. *Proc. Nat. Acad. Sci. USA* **84**, 1585-1589.
- Zucker-Franlin, D.** (1980). Eosinophil structure and maturation. In *The Eosinophil in Health and Disease* (ed. A. A. Mahmoud, K. F. Austen and A. S. Simon), pp. 43-59. New York: Grune and Stratton.

(Received 9 July, 1992 - Accepted 8 October, 1992)

